

1 Nanopore sequencing for the detection and the
2 identification of *Xylella fastidiosa* subspecies and sequence
3 types from naturally infected plant material

4
5 Luigi Faino^{1*}, Valeria Scala², Alessio Albanese¹, Vanessa Modesti², Alessandro Grottoli¹, Nicoletta
6 Pucci², Alessia L'Aurora², Massimo Reverberi¹, Stefania Loreti^{2*}

7 ¹ Department of Environmental Biology, University of Rome, Sapienza, P.le Aldo Moro, 5, Roma, 00185,
8 Italy

9 ² Consiglio per la Ricerca in Agricoltura e l'Analisi dell'Economia Agraria, Centro di Ricerca Difesa e
10 Certificazione, Via C.G. Bertero, 22, Rome, 00156, Italy

11 * Corresponding author:

12 Luigi Faino: luigi.faino@uniroma1.it;

13 Università degli Studi di Roma "La Sapienza", Dipartimento di Biologia Ambientale, p.le Aldo Moro 5,
14 Rome, 00185; Phone and Fax: +390649912433

15 Stefania Loreti: stefania.loreti@crea.gov.it

16 Consiglio per la Ricerca in Agricoltura e l'Analisi dell'Economia Agraria, Centro di Ricerca Difesa e
17 Certificazione, Via C.G. Bertero, 22, Rome, 00156, Italy; Phone +390682070341; Fax +390686802296

18 Running title:

19 *X. fastidiosa* detection by Nanopore sequencing

20 Keywords:

21 *Xylella fastidiosa*, MinION, pathogen detection

22

23

24 **Originality Significance Statement**

25 In this work we developed a methodology that allows the detection and identification of *Xylella*
26 *fastidiosa* in plant using the Nanopore technology portable device MinION. The approach that we
27 develop resulted more sensitive than methods currently used for detecting *X. fastidiosa*, like real-
28 time PCR. This approach can be extensively used for *X. fastidiosa* detection and it may pave the
29 road for the detection of other tedious vascular pathogens.

30

31

32 **Summary**

33 *Xylella fastidiosa* (*Xf*) is a polyphagous gram-negative bacterial plant pathogen that can infect more
34 than 300 plant species. It is endemic in America while, in 2013, *Xf* subsp. *pauca* was for the first
35 time reported in Europe on olive tree in the Southern Italy. The availability of fast and reliable
36 diagnostic tools is indispensable for managing current and future outbreaks of *Xf*.

37 In this work, we used the Oxford Nanopore Technologies (ONT) device MinION platform for
38 detecting and identifying *Xf* at species, subspecies and Sequence Type (ST) level straight from
39 infected plant material. The study showed the possibility to detect *Xf* by direct DNA sequencing and
40 identify the subspecies in highly infected samples. In order to improve sensitivity, Nanopore
41 amplicon sequencing was assessed. Using primers within the set of the seven MLST officially
42 adopted for identifying *Xf* at type strain level, we developed a workflow consisting in a multiple
43 PCR and an *ad hoc* pipeline to generate MLST consensus after Nanopore-sequencing of the
44 amplicons. The here-developed combined approach achieved a sensitivity higher than real-time
45 PCR allowing within few hours, the detection and identification of *Xf* at ST level in infected plant
46 material, also at low level of contamination.

47

48 **Introduction**

49 *Xylella fastidiosa* (*Xf*), a gram-negative phytopathogenic bacterium (Wells *et al.*, 1987), has
50 a very broad host range, causing different diseases in important crops (Hopkins, 1989) and in many
51 urban shade trees (Sherald and Kostka, 1992). *Xf* symptoms may not be evident and many hosts are
52 symptomless making this pathogen very difficult to manage. The pathogen is transmitted by xylem
53 sap feeding insects and colonizes the host xylem vessel, causing the typical leaf scorching. *Xf* is an
54 endemic pathogen in America and only recently was identified in southern Italy on olive trees
55 (Saponari *et al.*, 2013), in Corsica and in the south-east Mediterranean coast of France on several
56 hosts (Denancé *et al.*, 2019). Subsequently, records of *Xf* were reported in Germany on oleander
57 (EPPO, 2016a) and in Spain, Mallorca Island and Andalusia, on different plant species (Landa,
58 2017; Olmo *et al.*, 2017). Recently, a new finding was also reported in Tuscany (Marchi *et al.*,
59 2018). Different *Xf* subspecies were identified in Europe in association to the above-mentioned
60 natural outbreaks and interceptions on ornamental plants. There are three formally accepted
61 subspecies of *Xf*, i.e. *fastidiosa*, *pauca* and *multiplex*, based on DNA–DNA hybridization, as
62 recently confirmed by comparative genomic analysis (Schaad *et al.*, 2002; Marcelletti and
63 Scortichini, 2016; Denancé *et al.*, 2019). However, the International Society of Plant Pathology
64 Committee on the Taxonomy of Plant Pathogenic Bacteria (ISPP-CTPPB) considered valid names
65 only the subsp. *fastidiosa* and subsp. *multiplex* whereas other authors classified five subspecies
66 (*fastidiosa*, *pauca*, *multiplex*, *sandyi* and *morus*) (Bull *et al.*, 2012; Nunney *et al.*, 2012).
67 Complicating the whole taxonomic scenario, *Xf* subspecies includes different sequence types (ST)
68 which are determined by Multi Locus Sequence Typing (MLST) analysis based on the Sanger
69 sequencing technology of seven housekeeping gene (Yuan *et al.*, 2010; Nunney *et al.*, 2012; EPPO,
70 2016b). MLST analysis is recommended for new findings for the undoubtful identification of the
71 subspecies and ST in case of new outbreak or new plant hosts (EPPO, 2016b). Since the isolation of

72 *Xf* is tedious, the MLST analysis can be performed directly from DNA of the host plant; however,
73 low concentration of the bacteria and contaminants derived from the plant material makes the
74 MLST amplification, thus ST determination, extremely challenging.

75 Currently, next generation sequencing (NGS) platforms represent high throughput
76 technologies which allow obtaining large datasets of genetic information. In biomedical field,
77 sequencing technologies are rapidly being adopted for bacterial outbreak investigations (Faria *et al.*,
78 2017) and for rapid clinical diagnostics (Votintseva *et al.*, 2017). A combination of whole
79 transcriptome amplification and Nanopore sequencing device has been used to detect ‘*Candidatus*
80 *Liberibacter asiaticus*’ or plum pox virus in plants and insect vectors (Bronzato Badial *et al.*, 2018).
81 The reliability of Nanopore for the diagnosis of several plant pathogen was demonstrated
82 (Chalupowicz *et al.*, 2019) and a rapid MLST determination method was described for ST
83 estimation of *Klebsiella pneumoniae* isolates by the ONT MinION device (Page and Keane, 2018).

84 Direct Nanopore sequencing and Nanopore amplicon sequencing of two or seven
85 housekeeping genes were assessed on naturally infected and spiked samples. Additionally, a
86 consensus was generated from all seven MLST using amplicons sequenced by MinION device.
87 Nanopore amplicon sequencing provides the possibility, within few hours, to detect and identify *Xf*,
88 its subspecies and ST with an equal or slightly better sensitivity than the usual methods of detection
89 and identification or *Xylella* spp. such as real-time PCR.

90

91

92 **Results**

93 Detection and identification of *Xylella fastidiosa* in infected plant material by direct
94 Nanopore sequencing

95 Direct Nanopore sequencing was assessed to detect *Xf* in naturally infected plants by using the ONT
96 MinION device. The assay was firstly performed on DNA of 21 olive samples (dataset 1) and 7
97 samples of different plant species infected by *Xf* (dataset 2) for a total of 28 samples. All samples
98 were analysed by real-time PCR which revealed a variable level of infection among samples, e.g. in
99 samples of dataset 1, Ct ranged from 21.28 to 36.17, indicating a difference of about 10^5 times
100 between the most infected (Olive-1) and the less infected (Olive-11) sample (Tab. 1). The direct
101 Nanopore sequencing was developed in three experiments, the first one included samples Olive-1 to
102 Olive-12 (dataset 1), the second one, samples from Olive-13 to Olive-21 (dataset 1) and the third
103 experiment was composed of samples from different plant species (dataset 2) (Tab. 2). The first
104 flowcell generated ~3.2 Gb of data for 12 samples in 14 hours of run, the second flowcell produced
105 ~2.7 Gb for the remaining nine olive samples in ~30 hours while the last flowcell generated ~5.5
106 Gb in ~30 hours. All these flowcells were stopped before reaching the 48 hours run due to pore
107 saturation. The three subsets of samples were then subjected to independent de-barcoding and
108 analysis (see methods). After demultiplex of the samples, we were able to retain ~1.3 Gb (~40% of
109 the total reads) of data from the first subset of 12 samples, ~800 Mb (~30% of the total reads) for
110 the second subset while we got ~2 Gb of data for the samples from other plant species. The amount
111 of data for individual samples ranged from ~600 Mb in the *Cystus* sp. sample to ~10 Mb in Olive-
112 17 displaying a high variability between samples although we tried to use the same amount of input
113 gDNA (Tab. 1, 2). Each sample was analysed using a custom python script (called detection_script)
114 (see material and methods) in order to identify *Xf*. The analysis showed that each sample had a

115 similar bacterial composition and that *Xylella* was the most abundant genus (Tab. 1). Twenty-two
116 out of 28 samples showed reads that map uniquely to the genome of *Xylella* spp. It is worth of
117 mention, that all samples with more reads mapping to the *Xf* genome had a low Ct value (< 31),
118 suggesting that *Xf* can be detected only in heavily infected samples with the flowcell throughput
119 achieved in our work (Tab. 1). To better assess the performance of the direct Nanopore DNA
120 sequencing, we prepared 12 samples of uninfected olive DNA amended with a range of known
121 concentrations of DNA of *X. fastidiosa* subspecies *pauca* strain De Donno (CFBP 8402) (*Xfp*). The
122 amount of DNA was next or below the real-time PCR limit of detection, estimated around 10
123 fg/PCR reaction (Modesti *et al.*, 2017). Three samples (from LOD-10 to LOD-12) were not
124 detected by real-time PCR giving inconsistent results (Tab. 3). A new flowcell was used to
125 sequence these 12 samples generating ~667 Mb of data in 22 hours. The quantity of data/sample
126 ranged from 45 Mb to 7.7 Mb and *Xfp* was identified in four samples using the detection_script
127 (Tab. 3). These data confirm that Nanopore direct DNA sequencing can reliably detect *Xf* in
128 samples with a high bacterial concentration.

129 Nanopore amplicon sequencing

130 The MinION device generated about 290 Mb of data for all 12 samples (dataset 3) and after reads
131 demultiplex, we retained ~155 Mb of data. The number of reads is in a range of 14,360 and 54,405
132 for LOD-10 and LOD-2, respectively (Tab. 4). The detection_script was used to detect *Xf* in all
133 samples. The results showed that the number of reads matching uniquely a bacterial genome varied
134 between 3.39% in sample LOD-9 and 50.53% in sample LOD-5 (Tab. 4). As expected, the most
135 abundant genera represented in the mapped reads, >95% of the reads mapped to *Xf* (Tab. 4, Fig. 1).
136 The only exception is the sample LOD-9 for which low number of reads mapped to bacterial
137 genomes suggesting a problem in the sample preparation (Tab. 4, Fig. 1). The reduction of
138 sequencing error – since the same region is sequenced more than once - produces a more accurate
139 output allowing us to identify *Xf* at the subspecies level. To validate this, we used the

140 detection_script in combination with a specific *Xf* database formed by every *Xf* genome available at
141 the NCBI database (~60 genomes). The results showed that all 11 samples positive for *Xf* had >95%
142 of the reads correctly mapped to a genome identified as *Xf* subsp. *pauca* which is the subspecies
143 amended to the olive gDNA (Fig. 2). The same approach was used – amplification of *cysG* and
144 *malF*, Nanopore sequencing, querying the *Xf*-customised database – with the dataset 2 composed of
145 gDNA from different *Xf* naturally infected plant species (Tab. 5, Fig. 3). The results showed that for
146 all samples, except for *Rhamnus alaternus*, more than half of the reads mapped to *Xf*. Additionally,
147 the analysis using the specific *Xf* database showed that >90% of the reads mapped to *Xf* subsp.
148 *multiplex* genome (Fig. 3). To further support the subspecies identification results in the unknown
149 samples, we generated a consensus for the *cysG* and *malF* sequences using the consensus_script.
150 These consensus sequences were aligned to the *Xf* specific database matching 100% to *multiplex*
151 subspecies. This device correctly identify the *Xf* subspecies *multiplex* associated to the Tuscany
152 samples, according to the recent report of Marchi *et al.* (2018).

153 Identification of *Xylella* sequence-type using Nanopore amplicon sequencing

154 MLST consensus for all seven sequences for three (*Cystus* sp., *Rosmarinus officinalis*,
155 *Lavandula* sp.) out of the seven samples within the dataset 3 was generated using both Sanger and
156 Nanopore sequencing. These plant species were selected because the ST of *Xf* had not already been
157 determined. The consensus_script was used to generate a consensus using only Nanopore errors-
158 prone reads. As expected, the script generated seven sequences for each sample that were compared
159 with the same sequences generated by Sanger technology (Yuan *et al.*, 2010) followed by querying
160 the database at <http://pubmlst.org/xfastidiosa/> (Jolley *et al.*, 2018). Pairwise alignment of
161 concatenated sequences of all seven MLST derived from Sanger and Nanopore consensus resulted
162 in a 100% identity (Fig. 4). Additionally, when was compared the concatenated sequences from
163 both Sanger and Nanopore consensus sequences to the *Xf* MLST database, was found that samples
164 of *Cystus* sp., *Rosmarinus officinalis* and *Lavandula* sp. were infected by the ST 87 (Fig. 4). This

165 result is in agreement with recent findings of Xf ST 87 in *Prunus amygdalus*, *Polygala myrtifolia*,
166 *Spartium junceum* and *Rhamnus alaternus* (Saponari *et al.*, 2019).

167

168 **Discussion**

169 In the last fifteen years, NGS transformed genomic research with an inevitable impact also on
170 diagnostics, taking us to a new scenario. These technologies have recently been applied for the
171 diagnosis of plant pathogens (Bronzato Badial *et al.*, 2018; Chalupowicz *et al.*, 2019) and for the
172 detection and identification of *Xf* (Bonants *et al.*, 2019). Although several diagnostic methods are
173 available for the detection of *Xf* (EPPO, 2016b), the identification of subspecies and ST are
174 currently laborious and time-consuming. Recently, a tetraplex qPCR assays was developed for
175 simultaneous detection and identification of subspecies in plant tissues (Enora *et al.*, 2019). The
176 detection of *Xf* at subspecies level is fundamental and in case of new outbreaks or new plant hosts,
177 the identification of the ST is strongly recommended (EPPO Standard PM7/24 (4)). To circumvent
178 the complexity of the detection and identification of *Xf* subspecies and ST, we investigate the use of
179 Oxford Nanopore Technologies (ONT) MinION device.

180 Direct Nanopore DNA sequencing was firstly assessed by using naturally infected samples (dataset
181 1 and 2). One of the advantages of MinION device compared to other NGS platform is the
182 portability.

183 However, our results showed that only in highly infected samples *Xf* can be reliably detected and its
184 subspecies identified. All samples lacking reads mapping to the *Xf* genomes, showed a high Ct
185 value by real-time PCR that, associated to low throughput for these samples, made *Xf* undetectable.
186 This evidence was confirmed by using artificially spiked olive samples with DNA concentration of
187 *Xf* next and below the limit of detection of the real-time PCR (dataset 3), currently considered the
188 most sensitive assay for *Xf* detection (EPPO, 2016b; Modesti *et al.*, 2017). Nanopore direct DNA
189 sequencing of these samples provides a very low number of reads which reflect an even lower
190 number of reads mapping to *Xf* genomes making the analysis doubtful. A similar result was also
191 obtained by Bonants *et al.* (2019) using Illumina, who reported the ability of NGS to determine the

192 ST of *Xf* only in highly infected samples. The reason of the low sensitivity of the direct Nanopore
193 sequencing should be addressed to the low quality of the DNA for the tested samples. Nanopore
194 sequencing suffer of low throughput when the DNA used for the sequencing has contaminants
195 and/or when reads are shorts (Chalupowicz *et al.*, 2019). Further optimization of the DNA
196 purification and size selection step may be necessary to maximize the performance of the Nanopore
197 system. This aspect is of relevant importance because *Xf* has a very broad host-range and even using
198 the same extraction method, the DNA quality can be compromised by contaminants present in the
199 host matrix. However, carrying out massive analyzes cannot provide time-consuming or expensive
200 DNA purifications and generally neither the DNA concentration nor the DNA quality are
201 determined before a routinely analysis. Charalampous *et al.* (2019) developed a DNA extraction in
202 order to deplete host DNA from the samples and have more pathogen DNA. Using this approach,
203 they were able to identify respiratory pathogens in human samples. An alternative to sophisticated
204 DNA extraction methodology is amplicon sequencing (Kilianski *et al.*, 2015; Radhakrishnan *et al.*,
205 2019). This latter approach was assessed in order to overcome the low throughput of the flowcells
206 and to set up a more reliable and sensitive method, based on the amplification of two housekeeping
207 genes followed by Nanopore sequencing. Sequencing of *cysG* and *malF* for subspecies
208 discrimination is suggested by the EPPO Standard PM7/24 (4) and required, since 2018, in France
209 (Enora *et al.*, 2019). Nanopore amplicon sequencing was more efficacious than real-time PCR in *Xf*
210 detection of the spiked samples with low concentration of *Xf* target DNA (dataset 3, Tab. 3). These
211 results suggest that Nanopore amplicon sequencing has better sensitivity than real-time PCR. The
212 addition of the amplification step, even if lengthening the procedure, showed several advantages: *i*)
213 reduces the influence of DNA quality; *ii*) mitigates sequence error by repeatedly sequencing the
214 same region; *iii*) produces usable data faster than genomic DNA sequencing and *iv*) by using lower
215 stringency condition (40 cycles) in the amplification step, it obtains higher number of copies of the
216 target genes unusable for Sanger sequencing but exploitable for Nanopore sequencing (data not
217 shown).

218 The addition of the amplification allows in a single sequencing step the detection of the pathogen as
219 well as the identification of its subspecies and ST. The results of amplicon sequencing of the dataset
220 2 (Tab. 2) (*Spartium junceum*, *Polygala myrtifolia*, *Rosmarinus officinalis*, *Lavandula*, *Prunus*
221 *amygdalus*, *Cystus*) confirmed previous findings which identified as *multiplex* the subspecies
222 infecting these plants (Marchi *et al.*, 2018; Saponari *et al.*, 2019). These evidences showed that by
223 using an amplification step the method was able to detect and identify *Xf* in different plant species,
224 without interference due to the DNA quality.

225 The results obtained by amplicon sequencing of *cysG* and *malF* encourage us to test all the seven
226 housekeeping genes (*leuA*, *petC*, *malF*, *cysG*, *holC*, *nuoL*, *gltT*) to define the ST in our naturally
227 infected samples. For this purpose, Nanopore and Sanger sequencing of the seven housekeeping
228 genes were performed in *Lavandula* sp., *Rosmarinus officinalis* and *Cystus* sp. collected in Tuscany
229 Region, for which the ST has not yet been reported. Our results showed that *Xf* recovered from
230 these samples belong to the new ST 87 accordingly with previous findings on *Prunus amygdalus*,
231 *Polygala myrtifolia*, *Spartium junceum* and *Rhamnus alaternus* (Saponari *et al.*, 2019). The
232 simultaneous detection and identification of *Xf*, its subspecies and ST, developed in this study, lead
233 the Nanopore amplicon sequencing assay to be a powerful tool for a quick *Xf* diagnosis. The
234 evidences obtained in this study shows that the sequencing of two or seven housekeeping genes by
235 MinION is a promising alternative to detect and identify *Xf* from infected plant material, also in
236 low bacterial concentrations. This higher sensitivity is of interest for *Xf* detection in traded plants
237 and for latently infected material that represent one of the most serious threat for the dissemination.
238 For an “in field” application, further studies are required to make DNA direct Nanopore sequencing
239 reliable in detecting low concentration pathogens, i.e. using single flow-cells for the processing of
240 individual samples. This allows a greater depth in sequencing, with consequent higher possibility of
241 detection and identification of *Xf* /subspecies/STs. In conclusion, the evidences obtained in this
242 study paving the way for new opportunities of Nanopore sequencing as an effective surveillance
243 tool for *Xf* early detection.

244

245

246 **Experimental procedures**

247 Samples and DNA extraction

248 Sample preparation

249 Three datasets of samples were prepared as following: the first dataset (1) consists of twenty-one
250 DNA samples extracted from naturally infected olive plants (*Olea europea* L.) collected in Apulia
251 region (southern Italy) as described in Scortichini *et al.* (2018). The second dataset (2) consisted of
252 naturally infected samples of *Spartium junceum*, *Polygala myrtifolia*, *Rosmarinus officinalis*,
253 *Rhamnus alaternus*, *Prunus amygdalus*, *Cistus* and *Lavandula* spp., collected in Tuscany. The third
254 dataset (3) consists of DNA of healthy olives tree (collected in Latium) spiked with known quantity
255 of DNA of *Xfp* strain CFBP 8402. Plant DNA extraction of dataset 2 and 3 were performed by
256 CTAB-based method as reported in EPPO Standard PM7/ 24 (4).

257 A pure culture of *Xfp* strain CFBP 8402 was grown for seven days at 28° C in BYCE medium. The
258 culture scraped and resuspended in 100 µl of PBS, was grown in 10 ml of PD2 broth at 28° C, 170
259 rpm, for 7-10 days. The bacterial DNA was extracted from 700 µl of pure culture using the Gentra
260 Puregene Yeast/Bact Kit (Qiagen, The Netherlands). DNA (about 40 ng/µl) of healthy olive
261 samples was amended with 100, 10, 8, 4 fg/PCR reaction of *Xfp* DNA, each in three independent
262 replicates.

263

264 Real-time PCR and Multi-Locus Sequence Typing (MLST)

265 Datasets DNA were quantified by DS-11 FX+ spectrophotometer (DENOVIX) and diluted to a
266 final concentration of 20 ng/µL. *Xf* was detected in dataset 1 DNA by real-time PCR as described

267 by Harper *et al.* (2010) in a final volume of 10 µl and in datasets 2 and 3 by Francis *et al.* (2006).
268 All samples were also tested by Li *et al.* (2013) to confirm the bacterial infection. MLST analysis
269 was performed on *Cystus*, *Lavandula* and *Rosmarinus* as previously described (Yuan *et al.*, 2010;
270 EPPO, 2016b). Subspecie identification by sequencing *cysG* and *malF* was performed in dataset 2.
271 For Nanopore amplicon sequencing the amplification of housekeeping genes was modified
272 increasing the cycles of PCR condition from 35 to 40.

273 Datasets used for Nanopore sequencing

274 Direct Nanopore DNA sequencing was performed on the three previously described datasets (Tab.
275 1, 2, 3). Dataset 3 was used to test the direct DNA Nanopore sequencing in condition that was next
276 the limit of detection (LoD) of the real-time PCR (Tab. 3). DNA samples from dataset 2 and 3 were
277 used for Nanopore amplicon sequencing of the two genes, *cysG* and *malF*. Three out of seven
278 samples of the dataset 2 (i.e. *Cystus*, *Lavandula* and *Rosmarinus*) were assessed by Nanopore
279 amplicon sequencing of all seven housekeeping genes.

280 Nanopore sequencing

281 Nanopore sequencing libraries were prepared according to manufacture instruction for the kit SQK-
282 RBK004 for both direct DNA and amplicon sequencing. In brief, about ~400 ng of DNA was
283 purified using AMPure beads, ligated to the indexing adapter, combined in one sample and
284 subsequently ligated to the RAP adapter prior sequencing. For amplicon sequencing, PCR
285 amplicons of each sample were pulled together and purified using Isolate II PCR and gel Kit
286 (BIOLINE) and about 100 ng of DNA was used in library preparation. DNA samples were run on
287 the flowcell until pore life ended while amplicon sequencing runs were performed for shorted time
288 (~5hours). After sequencing, Deepbiner (v0.2.0)(Wick *et al.*, 2018) was used to de-multiples the
289 samples by default parameters. Subsequently, basecalling and a new run of demultiplex was

290 performed using Guppy (v2.3.1; default parameters)(Wick *et al.*, 2019). Deepbiner and guppy
291 basecalling were performed on a GPU card Nvidia GTX 1070 8Gb.

292

293 Pipeline for gDNA *Xylella* detection: detection_script

294 Reads generated by the two-step de-barcoding analysis were analysed using a custom pipeline. In
295 brief, reads were mapped to a database by using Minimap2 (v2.17-r941)((Li, 2018) software using -
296 -MD and --secondary=no as additionally parameters. The mapping is split in two steps: the first step
297 aligns all the reads against a database that includes one representative genome for all sequenced
298 bacterial species (about 10,500 bacterial genomes) present at the NCBI Genebank database and a
299 second step that align all reads mapped to *Xf* in the first step to a *Xf* specific database. The *Xf*
300 database it is formed by ~60 genomes. For both steps, alignment output files are parsed to retrieve
301 only the best match for reads mapping on multiple genomes. Finally, the number of reads mapping
302 on the same subspecies/strain are combine and summarized in plot
303 (<https://github.com/lfaino/xylella>).

304 MLST consensus generation: consensus_script

305 A second pipeline was written in order to generate MLST consensus after Nanopore sequencing.
306 Briefly, reads from Nanopore sequencing are demultiplexed by using Deepbiner software
307 (v0.2.0)(Wick *et al.*, 2018). Subsequently, porechop software (v0.2.4) is used to remove adapters
308 from the kept reads. Two rounds of reads correction by racon software (v1.3.3) (Vaser *et al.*, 2017)
309 are performed. The corrected reads are passed to jellyfish software (v2.2.8) (Marçais and Kingsford,
310 2011) and reads of 100 nt are generated. These reads are assembled by SPADES software (v3.12.0)
311 (Vyahhi *et al.*, 2012) and the assembled contigs polished by Nanopolish (v0.11.1) and subsequently
312 by bcftools mpileup software (v1.7.2) (Danecek and McCarthy, 2017). The reconstructed MLST

313 sequences are compared to all other MLST deposited at <https://pubmlst.org/> (Jolley *et al.*, 2018).

314 The script used for MLST reconstruction can be found at GitHub (<https://github.com/lfaino/xylella>).

315

316

317

318 **Acknowledgements**

319 This work was supported by MIPAAFT, Project Oli.Di.X.I.It (“OLivicoltura e Difesa da *Xylella*
320 *fastidiosa* e da Insetti vettori in Italia”), D.M. 23773 del 6/09/2017.

321

322

323

324

325 **References**

326 Bonants, P., Griekspoor, Y., Houwers, I., Krijger, M., van der Zouwen, P., van der Lee, T.A.J., and
327 van der Wolf, J. (2019) Development and Evaluation of a Triplex TaqMan Assay and Next-
328 Generation Sequence Analysis for Improved Detection of *Xylella* in Plant Material. *Plant Dis* **103**:
329 645–655.

330 Bronzato Badial, A., Sherman, D., Stone, A., Gopakumar, A., Wilson, V., Schneider, W., and King,
331 J. (2018) Nanopore Sequencing as a Surveillance Tool for Plant Pathogens in Plant and Insect
332 Tissues. *Plant Dis* **102**: 1648–1652.

333 Bull, C.T., De Boer, S.H., Denny, T.P., Firrao, G., Fischer-Le Saux, M., Saddler, G.S., et al. (2012)
334 List of new names of plant pathogenic bacteria (2008-2010). *J Plant Pathol* **94**: 21–27.

335 Chalupowicz, L., Dombrovsky, A., Gaba, V., Luria, N., Reuven, M., Beerman, A., et al. (2019)
336 Diagnosis of plant diseases using the Nanopore sequencing platform. *Plant Pathol* **68**: 229–238.

337 Charalampous, T., Kay, G.L., Richardson, H., Aydin, A., Baldan, R., Jeanes, C., et al. (2019)
338 Nanopore metagenomics enables rapid clinical diagnosis of bacterial lower respiratory infection.
339 *Nat Biotechnol* **37**: 783–792.

340 Danecek, P. and McCarthy, S.A. (2017) BCFtools/csq: haplotype-aware variant consequences.
341 *Bioinformatics* **33**: 2037–2039.

342 Denancé, N., Briand, M., Gaborieau, R., Gaillard, S., and Jacques, M.A. (2019) Identification of
343 genetic relationships and subspecies signatures in *Xylella fastidiosa*. *BMC Genomics* **20**..

344 Enora, D., Martial, B., Marie-Agnès, J., and Sophie, C. (2019) Novel tetraplex qPCR assays for
345 simultaneous detection and identification of *Xylella fastidiosa* subspecies in plant tissues. *bioRxiv*
346 699371.

347 EPPO (2016a) First report of *Xylella fastidiosa* in Spain. *EPPO Report Serv* **11**: 133.

348 EPPO (2016b) PM 3/81 (1) Inspection of consignments for *Xylella fastidiosa*. *EPPO Bull Stand* **46**:

349 395–406.

350 Faria, N.R., Quick, J., Claro, I.M., Theze, J., de Jesus, J.G., Giovanetti, M., et al. (2017)

351 Establishment and cryptic transmission of Zika virus in Brazil and the Americas. *Nature* **546**: 406.

352 Francis, M., Lin, H., Rosa, J.C.-L., Doddapaneni, H., and Civerolo, E.L. (2006) Genome-based

353 PCR primers for specific and sensitive detection and quantification of *Xylella fastidiosa*. *Eur J*

354 *Plant Pathol* **115**: 203–213.

355 Harper, S.J., Ward, L.I., and Clover, G.R.G. (2010) Development of LAMP and Real-Time PCR

356 Methods for the Rapid Detection of *Xylella fastidiosa* for Quarantine and Field Applications .

357 *Phytopathology* **100**: 1282–1288.

358 Hopkins, D.L. (1989) *Xylella Fastidiosa*: Xylem-Limited Bacterial Pathogen of Plants. *Annu Rev*

359 *Phytopathol* **27**: 271–290.

360 Jolley, K.A., Bray, J.E., and Maiden, M.C.J. (2018) Open-access bacterial population genomics:

361 BIGSdb software, the PubMLST. org website and their applications. *Wellcome open Res* **3**:

362 Kilianski, A., Haas, J.L., Corriveau, E.J., Liem, A.T., Willis, K.L., Kadavy, D.R., et al. (2015)

363 Bacterial and viral identification and differentiation by amplicon sequencing on the MinION

364 nanopore sequencer. *Gigascience* **4**:

365 Landa, B.B. (2017) Emergence of *Xylella fastidiosa* in Spain: current situation.

366 Li, H. (2018) Minimap2: Pairwise alignment for nucleotide sequences. *Bioinformatics* **34**: 3094–

367 3100.

368 Li, W., Levy, L., Teixeira, D.C., Lopes, S., Ayres, A.J., Hartung, J.S., et al. (2013) Development

369 and systematic validation of qPCR assays for rapid and reliable differentiation of *Xylella fastidiosa*

370 strains causing citrus variegated chlorosis. *J Microbiol Methods* **92**: 79–89.

371 Marçais, G. and Kingsford, C. (2011) A fast, lock-free approach for efficient parallel counting of

372 occurrences of k-mers. *Bioinformatics* **27**: 764–770.

373 Marcelletti, S. and Scortichini, M. (2016) Genome-wide comparison and taxonomic relatedness of

374 multiple *Xylella fastidiosa* strains reveal the occurrence of three subspecies and a new *Xylella*

375 species. *Arch Microbiol* **198**: 803–812.

376 Marchi, G., Rizzo, D., Ranaldi, F., Ghelardini, L., Ricciolini, M., Scarpelli, I., et al. (2018) First
377 detection of *Xylella fastidiosa* subsp. *multiplex* DNA in Tuscany (Italy). *Phytopathol Mediterr* **57**:
378 363–364.

379 Modesti, V., Pucci, N., Lucchesi, S., Campus, L., and Loreti, S. (2017) Experience of the Latium
380 region (Central Italy) as a pest-free area for monitoring of *Xylella fastidiosa*: distinctive features of
381 molecular diagnostic methods. *Eur J Plant Pathol* **148**: 557–566.

382 Nunney, L., Elfekih, S., and Stouthamer, R. (2012) The importance of multilocus sequence typing:
383 Cautionary tales from the bacterium *Xylella fastidiosa*. *Phytopathology* **102**: 456–462.

384 Olmo, D., Nieto, A., Adrover, F., Urbano, A., Beidas, O., Juan, A., et al. (2017) First Detection of
385 *Xylella fastidiosa* Infecting Cherry (*Prunus avium*) and *Polygala myrtifolia* Plants, in Mallorca
386 Island, Spain . *Plant Dis* **101**: PDIS-04-17-0590.

387 Page, A.J. and Keane, J.A. (2018) Rapid multi-locus sequence typing direct from uncorrected long
388 reads using Krocus . *PeerJ* **6**: e5233.

389 Radhakrishnan, G. V, Cook, N.M., Bueno-Sancho, V., Lewis, C.M., Persoons, A., Mitiku, A.D., et
390 al. (2019) MARPLE, a point-of-care, strain-level disease diagnostics and surveillance tool for
391 complex fungal pathogens. *BMC Biol* **17**: 1–17.

392 Saponari, M., Boscia, D., Nigro, F., and Martelli, G.P. (2013) Identification of dna sequences
393 related to *Xylella fastidiosa* in oleander, almond and olive trees exhibiting leaf scorch symptoms in
394 Apulia (Southern Italy). *J Plant Pathol* **95**: 668.

395 Saponari, M., D'Attoma, G., Kubaa, R.A., Loconsole, G., Altamura, G., Zicca, S., et al. (2019) A
396 new variant of *Xylella fastidiosa* subspecies *multiplex* detected in different host plants in the
397 recently emerged outbreak in the region of Tuscany, Italy. *Eur J Plant Pathol* 1–6.

398 Scally, M., Schuenzel, E.L., Stouthamer, R., and Nunney, L. (2005) Multilocus sequence type
399 system for the plant pathogen *Xylella fastidiosa* and relative contributions of recombination and
400 point mutation to clonal diversity. *Appl Environ Microbiol* **71**: 8491–8499.

401 Schaad, N.W., Opgenorth, D., and Gaush, P. (2002) Real-time polymerase chain reaction for one-
402 hour on-site diagnosis of Pierce's disease of grape in early season asymptomatic vines.
403 *Phytopathology* **92**: 721–728.

404 Sherald, J.L. and Kostka, S.J. (1992) Bacterial Leaf Scorch of Landscape Trees Caused By *Xylella*
405 *fastidiosa* 1. **18**: 57–63.

406 Vaser, R., Sović, I., Nagarajan, N., and Šikić, M. (2017) Fast and accurate de novo genome
407 assembly from long uncorrected reads. *Genome Res* **27**: 737–746.

408 Votintseva, A.A., Bradley, P., Pankhurst, L., Del Ojo Elias, C., Loose, M., Nilgiriwala, K., et al.
409 (2017) Same-day diagnostic and surveillance data for tuberculosis via whole-genome sequencing of
410 direct respiratory samples. *J Clin Microbiol* **55**: 1285–1298.

411 Vyahhi, N., Prjibelski, A.D., Nurk, S., Pyshkin, A. V., Dvorkin, M., Alekseyev, M. a., et al. (2012)
412 SPAdes: A New Genome Assembly Algorithm and Its Applications to Single-Cell Sequencing. *J*
413 *Comput Biol* **19**: 455–477.

414 Wells, J.M., Raju, B.C., Hung, H.-Y., Weisburg, W.G., Mandelco-Paul, L., and Brenner, D.J.
415 (1987) *Xylella fastidiosa* gen. nov., sp. nov: Gram-Negative, Xylem-Limited, Fastidious Plant
416 Bacteria Related to *Xanthomonas* spp. *Int J Syst Bacteriol* **37**: 136–143.

417 Wick, R.R., Judd, L.M., and Holt, K.E. (2018) Deepbinner: Demultiplexing barcoded Oxford
418 Nanopore reads with deep convolutional neural networks. *PLoS Comput Biol* **14**:

419 Wick, R.R., Judd, L.M., and Holt, K.E. (2019) Performance of neural network basecalling tools for
420 Oxford Nanopore sequencing. *Genome Biol* **20**: 129.

421 Yuan, X., Morano, L., Bromley, R., Spring-Pearson, S., Stouthamer, R., and Nunney, L. (2010)
422 Multilocus Sequence Typing of *Xylella fastidiosa* Causing Pierce's Disease and Oleander Leaf
423 Scorch in the United States . *Phytopathology* **100**: 601–611.

424

425

426

427

428

429 **Tables**

430 Table 1) Direct Nanopore sequencing of DNA of *Xylella fastidiosa* naturally infected olives
 431 samples collected in Apulia region (Dataset 1).

Sample s	Ct ^a	Mbases	# reads	# reads mapped (%) ^b	# reads mapped on Bacteria (%) ^c	# reads mapping to <i>Xylella fastidiosa</i> (%) ^d
Olive-1	21.28	140.47	46,444	41,478 (89.3)	755 (1.8)	111 (14.7)
Olive-2	21.44	227.67	80,039	70,081 (87.6)	1,236 (1.8)	188 (15.2)
Olive-3	21.92	113.07	34,789	31,012 (89.1)	556 (1.8)	49 (8.8)
Olive-4	25.7	100.87	44,308	39,342 (88.8)	539 (1.4)	5 (0.9)
Olive-5	25.5	62.23	33,632	28,633 (85.1)	367 (1.3)	3 (0.8)
Olive-6	25.3	68.11	33,152	28,773 (86.8)	384 (1.3)	6 (1.6)
Olive-7	27.85	107.05	39,608	34,853 (88.0)	537 (1.5)	9 (1.7)
Olive-8	27.24	95.05	33,240	29,871 (89.9)	525 (1.8)	2 (0.4)
Olive-9	27.74	102.02	39,916	35,393 (88.7)	580 (1.6)	12 (2.1)
Olive-10	35.3	43.94	17,468	15,383 (88.1)	213 (1.4)	0 (0.0)
Olive-11	36.17	160.30	52,157	46,588 (89.3)	827 (1.8)	0 (0.0)
Olive-12	35.06	43.47	18,259	15,689 (85.9)	249 (1.6)	0 (0.0)
Olive-13	28	69.15	30,135	25,379 (84.2)	325 (1.3)	4 (1.2)
Olive-14	26	111.75	42,884	37,284 (86.9)	538 (1.4)	61 (11.3)
Olive-15	34.5	87.21	34,260	29,717 (86.7)	448 (1.5)	1 (0.2)
Olive-16	33.75	94.79	42,478	36,246 (85.3)	480 (1.3)	0 (0.0)
Olive-17	31.6	31.19	10,868	9,586 (88.2)	131 (1.4)	0 (0.0)
Olive-18	30.1	101.70	43,913	37,632 (85.7)	475 (1.3)	3 (0.6)
Olive-19	25.3	81.98	28,591	24,781 (86.7)	402 (1.6)	22 (5.5)
Olive-20	36	128.11	37,611	33,844 (90.0)	543 (1.6)	0 (0.0)
Olive-21	29	106.21	35,496	31,236 (88.0)	540 (1.7)	4 (0.7)

432

433 ^a Cycle threshold obtained by Harper *et al.*, 2010, TaqMan version

434 ^b Percentage of reads mapped to bacterial genomes and *Oleae europaea* over the number of total reads sequenced

435 ^c Percentage of reads mapped to bacterial genomes and *Oleae europaea* from the total mapped

436 ^d Percentage of reads mapped on *Xylella fastidiosa* genomes over the number of reads mapped to Bacterial genomes

437

438

439

440 Table 2) Direct Nanopore sequencing of DNA of *Xylella fastidiosa* naturally infected plant samples
 441 collected from Tuscany Region (dataset 2)

442

Samples	Ct ^a	Mbases	# reads	# reads mapped (%) ^b	# reads mapped on Bacteria (%) ^c	# reads mapping to <i>Xylella fastidiosa</i> (%) ^d
<i>Prunus dulcis</i>	27,35	122.78	114,327	11,508 (10.1)	7,621 (66.2)	22 (0.3)
<i>Rhamnus alaternus</i>	NA	73.45	62,664	4,335 (6.9)	2,737 (63.1)	10 (0.4)
<i>Cystus</i>	25,78	606.32	199,423	5,156 (2.6)	3,522 (68.3)	230 (6.5)
<i>Rosmarinus officinalis</i>	35,14	247.79	182,831	9,657 (5.3)	4,662 (48.3)	2 (0.1)
<i>Lavandula</i>	28,75	438.39	211,320	25,197 (11.9)	10,231 (40.6)	86 (0.8)
<i>Polygala myrtifolia</i>	25,10	184.91	87,762	11,447 (13.0)	6,157 (53.8)	104 (1.7)
<i>Spartium juceum</i>	18,61	286.19	155,150	10,919 (7.0)	6,650 (60.9)	1,699 (25.5)

443

444 ^a Cycle threshold obtained by Francis *et al.*, 2006, TaqMan version

445 ^b Percentage of reads mapped to bacterial genomes and *Oleae europaea* over the number of total reads sequenced

446 ^c Percentage of reads mapped to bacterial genomes and *Oleae europaea* from the total mapped

447 ^d Percentage of reads mapped on *Xylella fastidiosa* genomes over the number of reads mapped to bacterial genomes

448

449

450

451

452

453 Table 3) Direct Nanopore sequencing of healthy olives samples DNA spiked with known DNA
 454 concentrations of *Xylella fastidiosa* subsp. *pauca* strain De Donno (CFBP 8402) DNA (Dataset 3)

Samples	Ct ^a	<i>Xf</i> DNA [fg/μl]	fg gDNA ^b	Mbases	# reads	# reads mapped (%) ^c	#reads mapped on Bacteria (%) ^d	# reads mapping to <i>Xylella fastidiosa</i> (%) ^e
LOD-1	31.50-32.30	100 fg/μl	700fg	33.63	21,218	16,334 (77.0)	615 (3.8)	2 (0.3)
LOD-2	31.03-31.30	100 fg/μl	700fg	7.97	6,656	3,853 (57.9)	105 (2.7)	0 (0.0)
LOD-3	31.22-30.70	100 fg/μl	700fg	17.51	16,237	8,820 (54.3)	308 (3.5)	1 (0.3)
LOD-4	34.54-34.39	10 fg/μl	70fg	26.35	22,475	15,047 (66.9)	542 (3.6)	0 (0.0)
LOD-5	33.12-33.56	10 fg/μl	70fg	26.31	21,669	14,915 (68.8)	486 (3.3)	1 (0.2)
LOD-6	33.18-34.00	10 fg/μl	70fg	31.99	24,385	16,836 (69.0)	597 (3.5)	0 (0.0)
LOD-7	37.31-44	8 fg/μl	56fg	27.69	21,949	14,693 (66.9)	475 (3.2)	0 (0.0)
LOD-8	35-35.5	8 fg/μl	56fg	35.64	34,572	23,594 (68.2)	725 (3.1)	0 (0.0)
LOD-9	40-42	8fg/ul	56fg	22.15	29,800	18,724 (62.8)	455 (2.4)	0 (0.0)
LOD-10	37.40-NA [#]	4 fg/μl	28fg	39.51	38,724	26,887 (69.4)	740 (2.8)	1 (0.1)
LOD-11	36-NA [#]	4 fg/μl	28fg	45.19	45,824	30,053 (65.6)	833 (2.8)	0 (0.0)
LOD-12	41-NA [#]	4 fg/μl	28gf	10.07	21,082	10,627 (50.4)	272 (2.6)	0 (0.0)

455

456 ^a Cycle threshold obtained by Francis *et al.*, 2006, TaqMan version The value reports the Ct interval for the 3 technical
 457 replicates used for each sample. Low concentrate samples gave technical replicates with no Ct value

458 ^b Total amount of *X. fastidiosa* subspecies *pauca* gDNA added to *Oleae europaea* gDNA and used for Nanopore
 459 sequencing

460 ^c Percentage of reads mapped to bacterial genomes and *Oleae europaea* over the number of total reads sequenced

461 ^d Percentage of reads mapped to bacterial genomes and *Oleae europaea* from the total mapped

462 ^e Percentage of reads mapped on *Xylella fastidiosa* genomes over the number of reads mapped to bacterial genomes

463

464

465

466 Table 4) Nanopore amplicon sequencing of *cysG* and *malF* from DNA of healthy olives samples
 467 spiked with known amount of *Xylella fastidiosa* subsp. *pauca* strain De Donno (CFBP 8402) DNA
 468 (Dataset 3)

Samples	Ct ^a	Xf DNA [fg/ul]	Mbases	# reads	#reads mapped on Bacteria (%) _b	# reads mapping to <i>Xylella fastidiosa</i> (%) ^c
LOD-1	31.50-32.30	100 fg/μl	1.95	42,384	16,543 (39.0)	16,367 (98.9)
LOD-2	31.03-31.30	100 fg/μl	2.50	54,405	26,119 (48.0)	25,870 (99.0)
LOD-3	31.22-30.70	100 fg/μl	1.00	21,805	7,765 (35.6)	7,689 (99.0)
LOD-4	34.54-34.39	10 fg/μl	1.37	29,806	12,039 (40.4)	11,866 (98.6)
LOD-5	33.12-33.56	10 fg/μl	1.72	37,384	18,827 (50.4)	18,683 (99.2)
LOD-6	33.18-34.00	10 fg/μl	1.89	40,984	7,347 (17.9)	7,163 (97.5)
LOD-7	37.31-44	8 fg/μl	1.04	22,675	3,147 (13.9)	2,794 (88.8)
LOD-8	35-35.5	8 fg/μl	1.02	22,087	5,403 (24.5)	4,669 (86.4)
LOD-9	40-42	8fg/ul	1.20	24,336	832 (3.4)	2 (0.2)
LOD-10	37.40-NA#	4 fg/μl	0.66	14,360	4,687 (32.6)	4,394 (93.7)
LOD-11	36-NA#	4 fg/μl	0.68	14,710	4,867 (33.1)	4,659 (95.7)
LOD-12	41-NA#	4 fg/μl	1.21	26,334	12,336 (46.8)	12,124 (98.3)

469

470 ^a Cycle threshold obtained by Francis et al., 2006, TaqMan version

471 ^b percentage of reads mapped to Bacterial genomes over the number of total reads sequenced

472 ^c percentage of reads mapped on *Xylella fastidiosa* genomes over the number of reads mapped to Bacterial genomes

473 [#] the value reposts the Ct interval for the 3 technical replicates used for each samples. Low concentrate samples gave
 474 technical replicates with no Ct value

475

476

477

478

479

480

481 Table 5) Nanopore-amplicon-sequencing of *cysG* and *malF* from DNA of naturally infected plants
482 samples collected in Tuscany region

483

Samples	Ct ^a	Mbases	# reads	# reads mapping to <i>Xylella fastidiosa</i> (%) ^b
<i>Prunus dulcis</i>	27,35	0.28	6,108	3,396 (55.6)
<i>Rhamnus alaternus</i>	NA	0.44	9,462	28 (0.3)
<i>Cystus</i>	25,78	0.44	9,600	5,656 (58.9)
<i>Rosmarinus officinalis</i>	35,14	0.29	6,228	2,178 (35.0)
<i>Lavandula</i>	28,75	1.19	25,798	10,391 (40.3)
<i>Polygala myrtifolia</i>	25,10	0.51	11,085	7,065 (63.7)
<i>Spartium juceum</i>	18,61	0.50	10,959	5,633 (51.4)

484

485 ^a Cycle threshold obtained by Francis et al., 2006, TaqMan version

486 ^b percentage of reads mapped on *Xylella fastidiosa* genomes over the number of total reads sequenced

487

488

489 **Figure legends**

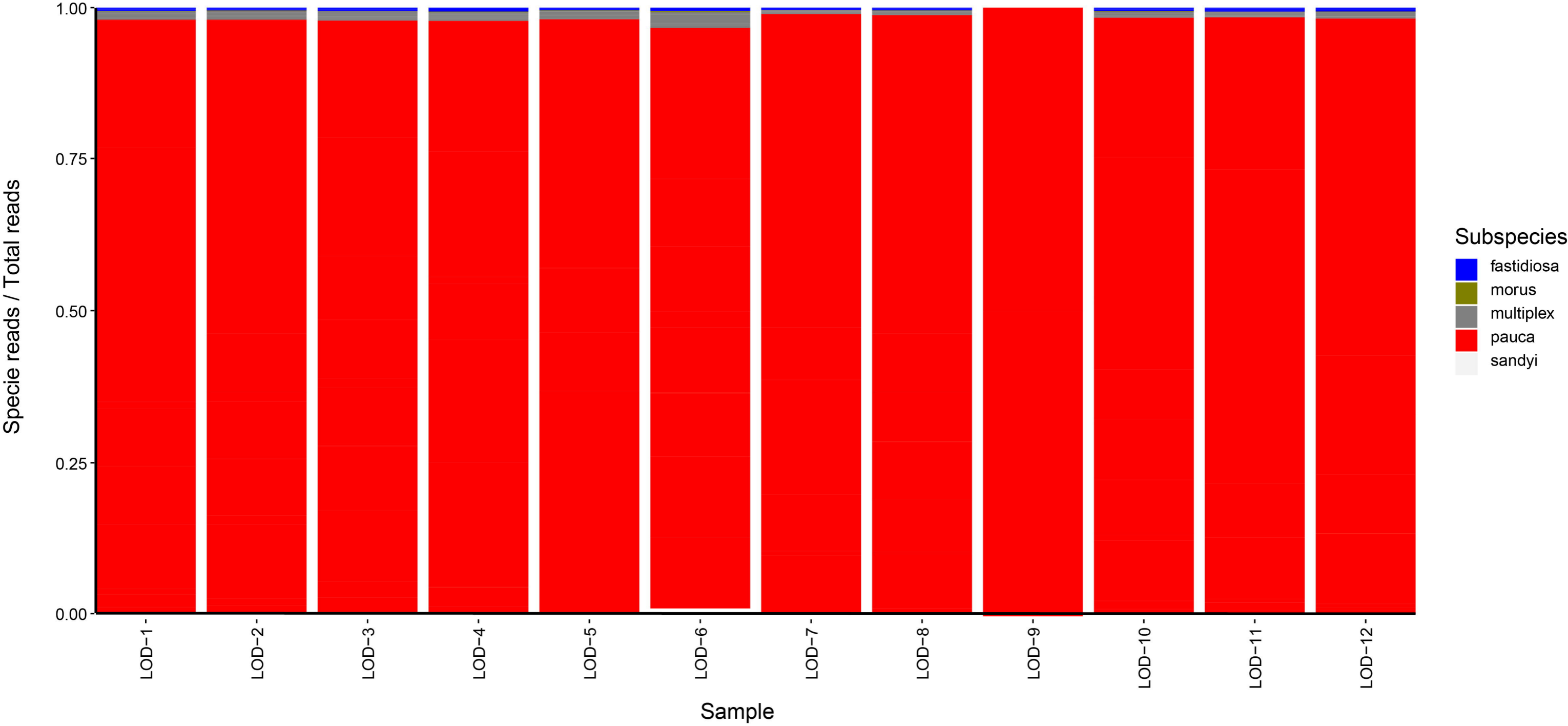
490 Figure 1) Stacked bar charts showing the actual relative abundance of bacterial families in the
491 identified using the detection_script on Nanopore ampliseq of olive DNA amended with different
492 amount of *X. fastidiosa* subspecies *pauca* DNA

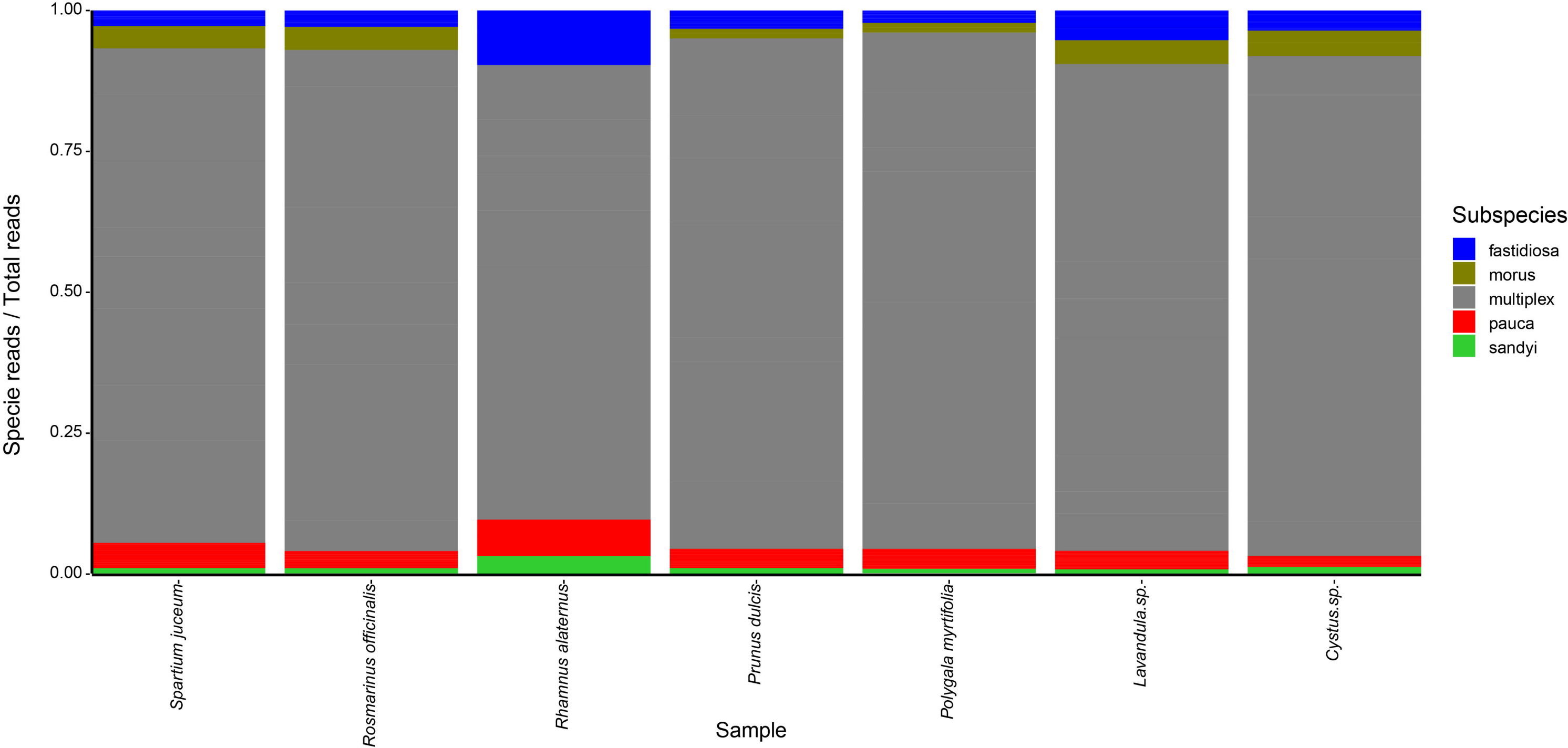
493 Figure 2) Stacked bar charts showing the actual relative abundance of *X. fastidiosa* subspecies *pauca*
494 compared to other *X. fastidiosa* subspecies using the detection_script on Nanopore ampliseq of
495 olive DNA amended with different amount of *X. fastidiosa* subspecies *pauca* DNA

496 Figure 3) Stacked bar charts showing the actual relative abundance of different *X. fastidiosa*
497 subspecies using the detection_script on Nanopore ampliseq of DNA from different plant species.
498 The highest subspecies present resulted to the *X. fastidiosa* subspecies *multiplex*

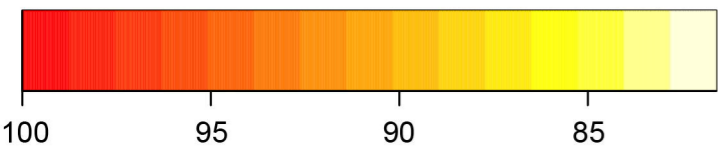
499 Figure 4) Heatmap representing sequence alignments of seven concatenated MLST for 87 ST
500 deposited at the MLST database (<https://pubmlst.org>), three sequences derived from Sanger
501 sequencing of *Rosmarinus officinalis*, *Cystus* sp. and *Lavandula* sp. and three sequences derived
502 from consensus of the Nanopore sequencing for *Rosmarinus officinalis*, *Cystus* sp. and *Lavandula*
503 sp. plant samples

504

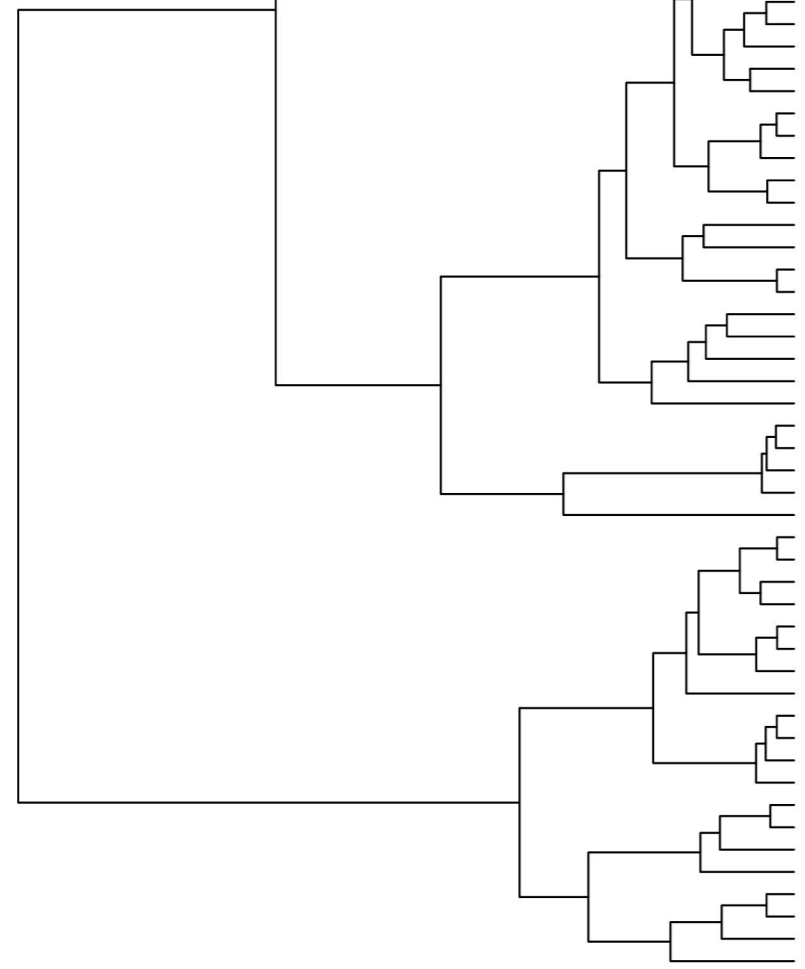
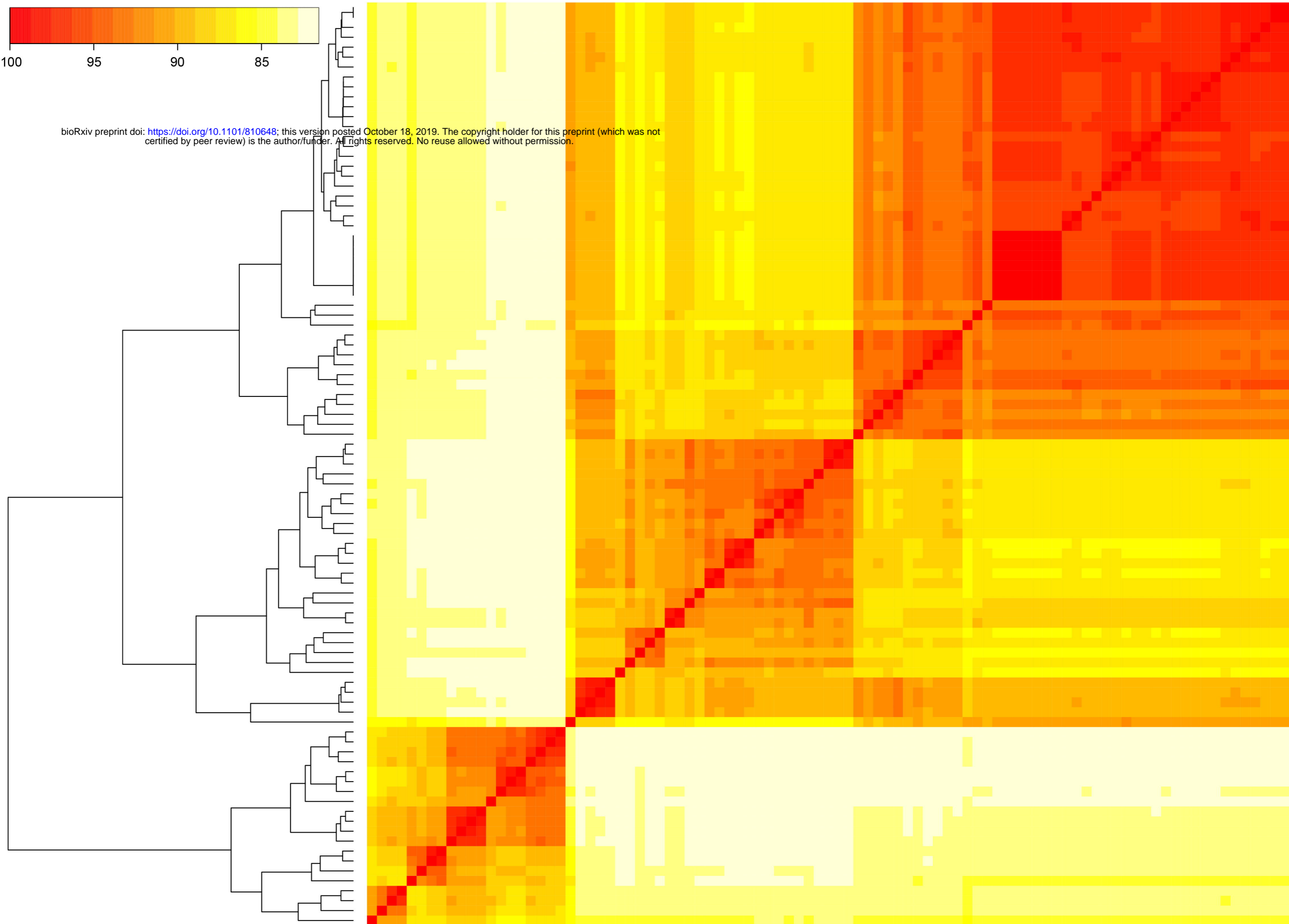




Percentage of similarity



bioRxiv preprint doi: <https://doi.org/10.1101/810648>; this version posted October 18, 2019. The copyright holder for this preprint (which was not certified by peer review) is the author/funder. All rights reserved. No reuse allowed without permission.



74 73 80 71 70 68 14 86 16 66 84 64 11 12 13 65 69 67 30 29 62 31 5 33 1 61 56 54 76 72 4 77 19 21 18 59 60 20 57 52 55 17 75 47 3 1 2 32 27 83 40 28 43 41 82 22 42 58 63 79 50 87
 Rosmarinus officinalis N
 Rosmarinus officinalis
 Cystus sp S
 Lavandula sp S
 Lavandula sp N
 Cystus sp N
 Rosmarinus officinalis N
 Lavandula sp N
 87 50 79 63 58 42 22 82 41 43 28 40 83 27 32 2 1 3 47 75 17 55 52 57 20 60 59 18 21 19 77 4 72 76 54 56 61 33 5 31 62 29 30 67 69 78 65 13 12 11 64 84 66 16 86 85 14 68 70 71 80 73 53 74

38
 24
 39
 8
 49
 23
 45
 34
 25
 35
 7
 81
 6
 10
 26
 36
 15
 46
 48
 37
 51
 44
 9
 Rosmarinus officinalis S
 Cystus sp S
 Lavandula sp S
 Cystus sp N
 Rosmarinus officinalis N
 Lavandula sp N

Lavandula sp N
 Rosmarinus officinalis
 Cystus sp
 Lavandula sp S
 Cystus sp
 Rosmarinus officinalis S
 9
 44
 51
 37
 48
 46
 15
 36
 26
 10
 6
 81
 35
 25
 34
 45
 23
 49
 8
 39
 24
 38